Gamma Knife Stereotactic radiotherapy combined with tislelizumab as later-line therapy in pMMR/MSS/MSI-L metastatic colorectal cancer: A Phase II Trial Analysis

Yiran Zhang[1,2*], Hanyang Guan[1*], Shijin Liu[1*], Haoquan Li[1], Zili Bian [1], Jiashuai He[1], Zhan Zhao[1], Shenghui Qiu[1], Tianmu Mo[1], Xiangwei Zhang[1], Zuyang Chen[1], Hui Ding[1], Xiaoxu Zhao[1], Liang Wang[3#], Yunlong Pan[1,4#], Jinghua Pan[1#]

1. Department of General Surgery, The First Affiliated Hospital of Jinan University, 510632, Guangzhou, Guangdong, P. R. China
2. Department of Body Gamma Knife, The First Affiliated Hospital of Jinan University, 510632, Guangzhou, Guangdong, P. R. China
3. Department of Oncology, The First Affiliated Hospital of Jinan University, 510632, Guangzhou, Guangdong, P. R. China
4. MOE Key Laboratory of Tumor Molecular Biology and Key Laboratory of Functional Protein Research of Guangdong Higher Education Institutes. Institute of Life and Health Engineering, Jinan University, Guangzhou, China.

*These authors contributed equally

Running title: Combined SBRT and Immunotherapy in pMMR mCRC.

[#]**Corresponding author:**
Jinghua Pan, Department of General Surgery, The First Affiliated Hospital of Jinan University, 510632, Guangzhou, Guangdong, P. R. China; E-mail: huajanve@foxmail.com
Yunlong Pan: Department of General Surgery, The First Affiliated Hospital of Jinan University, 510632, Guangzhou, Guangdong, P. R. China; E-mail: tpanyl@jnu.edu.cn
Liang Wang: Department of Oncology, The First Affiliated Hospital of Jinan University, 510632, Guangzhou, Guangdong, P. R. China. E-mail: wangliang@jnu.edu.cn.

Conflict of interest: The authors disclosed no potential conflicts of interest.

Abstract

An immunosuppressive tumor microenvironment limits the efficacy of immunotherapy, thus patients with MSS and pMMR mCRC often face great challenges.In this phase II trial, patients received Gamma Knife SBRT combined with Tislelizumab . P Biomarker analysis was performed pre- and post-treatment . From November 2022 to July 2024, 13 of 20 patients achieved PR, 6 achieved SD. mPFS was 10.7 months (95% CI, 6.4-15.0). With no grade 4 events noted, common adverse events included nausea (65%), anemia (55%), and fatigue (45%). For patients who had not responded to first and second-line therapies, the combo of Gamma Knife SBRT and tislelizumab showed high efficacy and reasonable safety. Significant post-radiotherapy improvements in the tumor's immunosuppressive microenvironment. These results imply that patients with pMMR/MSS/MSI-L mCRC who were unresponsive to the first and second-line chemotherapy, Gamma Knife SBRT with tislelizumab provides a safe and powerful later-line treatment alternative.

Keywords: Gamma Knife Stereotactic body radiation therapy; mismatch repair-proficient; tislelizumab; Metastatic colorectal cancer; Immune checkpoint inhibitors; PD-L1.

Statement of significance

This study offers a safe and powerful option for pMMR/MSS/MSI-L mCRC patients fail to first and second-line chemotherapy. And discover Gamma Knife SBRT contributed to potentially converting the suppressive "cold" tumor immune microenvironment into an activated "hot" microenvironment conducive to immunotherapy efficacy in pMMR CRC.

Introduction

Colorectal cancer continues to represent a significant threat to life. As reported in the 2020 Global Cancer Statistics, colorectal cancer accounts for 10% of all cancer cases, ranking third in incidence, while its mortality rate is 9.4%, second only to lung cancer (1,2). Especially, 20% of newly diagnosed colorectal cancer patients present show metastases, and 40% have recurrence and metastases after local treatment (3). The FOLFOX/FOLFIRI chemotherapy regimen, which comprises oxaliplatin, 5-fluorouracil, and irinotecan is the mainstay of clinical treatment for metastatic colorectal cancer (mCRC). For patients harboring wild-type RAS and BRAF, the addition of the epidermal growth factor receptor (EGFR) inhibitor cetuximab is recommended(4,5). For patients with RAS mutations, the anti-angiogenic agent bevacizumab is advised. Nevertheless, RAS-mutant patients exhibit poorer prognoses and shorter survival times compared to their wild-type counterparts (6,7). The efficacy of chemotherapy in combination with targeted therapy remains suboptimal (7).

The development of immune checkpoint inhibitors (ICIs) transforms cancer immunotherapy (8). Particularly CRCs with mismatch repair deficiency (dMMR) and high microsatellite instability (MSI-H) show a strong response to ICIs (9). But most CRC cases are either microsatellite-stable/low microsatellite instability (MSS/MSI-L) or mismatch repair-profile (pMMR), which reduces the efficacy of immunotherapy in a significant number of mCRC patients (9). Chemotherapeutic agents can cause immunogenic cell death in tumors, thus coordinating with ICIs improves anti-tumor efficacy (10). Additionally, anti-angiogenic therapies targeting VEGFR facilitate the normalization of tumor vasculature and promote immune cell infiltration, subsequently amplifying immune-mediated tumor eradication (11). Clinical studies, however, have revealed that t combining mFOLFOX6 or other

chemotherapy regimens with anti-VEGF, anti-EGFR, and ICIs does not produce better clinical outcomes in mCRC (12,13). Consequently, identifying alternative strategies to augment the efficacy of immunotherapy remains a pivotal objective in the field of cancer immunotherapy in pMMR/MSS/MSI-L mCRC.

Stereotactic body radiation therapy (SBRT), effectively targets and eradicates tumor cells with high-dose radiation (14). Although traditional radiotherapy is sometimes linked with immunosuppressive effects (15), SBRT's exact targeting can expose tumor neoantigens, mobilize and activate immune cells, increase their infiltration into the tumor, and improve the tumor immune microenvironment (16,17). The Gamma Knife is a principal modality in SBRT, employing gamma rays generated by cobalt-60 to deliver a single, high-dose focused irradiation to the target lesion. The Gamma Knife provides several benefits over conventional radiotherapy, including hiexact stereotactic targeting, increased delivery dose to the lesion, prevention of accelerated repopulation of tumor cells, and better local control rates of tumors(18). Our team firstly observed a case with pMMR-type mCRC who exhibited local recurrence and distant metastasis following first-line and second-line chemotherapy combined with targeted therapy(19). After undergoing gamma knife SBRT followed by tislelizumab treatment, intrahepatic metastatic lesions were reduced and stabilized, the patient showed a partial response (PR) with notable reduction of recurrent lesions in the rectal wall and stabilization of intrahepatic metastases, so extending the progression-free survival (PFS) exceeded beyond 3 months (19). These findings suggest that Gamma Knife SBRT might improve ICBs sensitivity in mCRC.

The results of a phase II clinical trial assessing the combination of Gamma Knife SBRT combined with tislelizumab as a later-line therapy in patients with pMMR/MSS/MSI-L mCRC are presented in this report together with safety and efficacy. NanoString assay for transcriptome analysis was employed to elucidate changes in the tumor immune microenvironment during the combined treatment, offering insights into the therapeutic potential and mechanistic underpinnings of this integrated approach.

Results

Patients

In this clinical trial, twenty patients with pMMR/MSS/MSI-L tumors refractory to first or second-line treatment were enrolled. The cohort comprised 15 males and 5 females, with ages ranging from 47 to 77 years. Predominantly, the primary tumors were located in the left colon and rectum (17/20, 85%), with the liver being the most common site of metastasis, followed by the lung (3/20)(**Table 1**). Flowchart of therapeutic regimen and flow diagram of enrolled participants in the study were shown in **Figure 1A** and **Figure 1B.**

Molecular profiling revealed RAS mutations in 11 patients (55%), with 5 exhibiting KRAS mutations and 6 presenting NRAS mutations. PD-L1 expression was assessed in 18 patients, 12 (60%) patients had combined positive score (CPS) ≤ 1. Tumor mutation burden (TMB) data were available for 8 patients, with a median TMB of 4.62 mutations/Mb (IQR 3.08-8.97). Notably, only one patient exhibited a TMB > 10 mutations/Mb (**Table 1)**.

Characteristics	Patients (n=20)
Age, years, median (IQR), n (%)	60 (56-65)
<60	8 (40%)
≥60	12 (60%)
Sex, n(%)	
Male	15 (75%)
Female	5 (25%)
ECOG performance status, n (%)	
0	12 (60%)
1	8 (40%)
Primary tumor location, n (%)	
Left colon and rectum	17 (85%)
Right colon	3 (15%)
Number of metastatic organs[a], n (%)	
1	14 (70%)
≥2	6 (30%)
Metastatic organ, n (%)	
Liver	14 (70%)
Lung	7 (35%)
Lymph node	2 (10%)
Other	3 (15%)
Ras mutation type, n (%)	
KRAS	5 (25%)
NRAS	6 (30%)
Other	9 (45%)
PD-L1 expression, CPS, n (%)	
CPS≤1	12 (60%)
CPS > 1	6 (30%)
Unknown	2 (10%)
TMB (mut/Mb), median (IQR), n (%)	4.62 (3.08-8.97)
TMB<5	4 (20%)
TMB≥5, ≤10	3 (15%)
TMB>10	1 (5%)
Unknown	12 (60%)

Abbreviations: CPS, combined positive score; ECOG, Eastern Cooperative Oncology Group; IQR, interquartile range; TMB, tumor mutation burden.

[a]Multiple answers allowed.

Table 1: Baseline demographic and clinical characteristics.

Efficacy

In our cohort of 20 patients meeting inclusion criteria, 13 (65%) achieved a partial response (PR), and 6 (35%) maintained stable disease (SD), resulting in a robust disease control rate (DCR) of 95% (**Table 2**). Patients with liver metastases achieved 92.9% DCR, and patients with metastases in non-liver locations notably achieved a remarkable 100% DCR, only 1 patient with liver metastases experienced disease progression (PD) (**Figure 2A**), As of the data cutoff date, 7 patients remained on maintenance treatment, and 1 patient underwent surgery due to disease progression (**Figure 2A**). Remarkably, 3 patients refractory to first-line treatment responded to SBRT combined with tislelizumab, achieving rapid regression to NED status, with durations ranging from 6 to 18 months before progression. Encouragingly, 1 patient remains in a state of NED, under ongoing monitoring (**Figure 2A**).

	All patients (N = 20)	**Liver metastasis (N = 14)**	**Other metastasis (N = 6)**
Best overall response			
Complete response (CR), n (%)	0 (0%)	0 (0%)	0 (0%)
Partial response (PR), n (%)	13 (65%)	8 (57%)	5 (83%)
Stable disease (SD), n (%)	6 (30%)	5 (36%)	1 (17%)
Progressive disease (PD), n (%)	1 (10%)	1 (7%)	0 (0%)
ORR, n (%, 95% CI)	13 (65%, 40.8-84.6%)	8 (57.1%, 28.9-82.3%)	5(83.3%, 35.9-99.6%)
DCR, n (%, 95% CI)	19 (95%, 75.1-99.9%)	13 (92.9%, 66.1-99.8%)	6(100%, 54.1-100%)

Abbreviations: ORR, objective response rate; DCR, disease control rate.

Table 2: Efficacy outcomes.

Most patients exhibited favorable survival outcomes throughout the treatment (**Figure 2B**), and median progression-free survival (PFS) was 10.7 months (95% CI, 6.4, 15.0) (**Figure 2C**). Additionally, a comparative survival analysis included 23 patients who underwent first and second-line treatment and Gamma Knife SBRT without immunotherapy, revealing a median PFS of 6.7 months (95% CI, 5.6, 7.0), this data shown Gamma Knife SBRT combined with tislelizumab as later-line treatment prolong PFS in mCRC (Log-rank test = 5.638, P = 0.0176) (**Figure 2D**). These findings suggest Gamma Knife SBRT combined with tislelizumab can effectively inhibiting mCRC progression.

In light of the abscopal effect of radiotherapy, we extended our observations beyond the lesions directly targeted by stereotactic radiotherapy to include non-irradiated lesions. Imaging examinations revealed significant tumor regression in both the irradiated target lesions (**Figure 2E, F**) and the non-irradiated lesions (**Figure 2E, G**) following Gamma Knife SBRT combined with tislelizumab. These findings suggest that SBRT not only impacts the irradiated lesions but also sensitize distant metastatic sites for ICBs through the abscopal effect, thereby enhancing the systemic antitumor response when combined with immunotherapy.

Safety

All 20 enrolled patients received the assigned treatment regimen, with safety assessments conducted every three treatment cycles. Treatment-related adverse events (TRAEs) and

immune-related adverse events are summarized in **Table 3.** Predominantly, patients experienced mild to moderate adverse events, with the most common being nausea (65%), anemia (55%), electrolyte disturbances (55%), fatigue (45%), and anorexia (35%). Notably, only two patients experienced grade 3 events of increased blood bilirubin, while no grade 4 adverse events were reported throughout the study period.

TEAEs, n (%)	**Patient (N=20)**				
	Grade 1	Grade 2	Grade 3	Grade 4	Any grade
Anemia	9 (45%)	2 (10%)	0	0	11 (55%)
Neutropenia	1 (5%)	0	0	0	1 (5%)
Nausea	10 (50%)	3 (15%)	0	0	13 (65%)
Poor appetite	3 (15%)	4 (20%)	0	0	7 (35%)
Electrolyte disturbance	7 (35%)	2 (10%)	0	0	11 (55%)
Hand-foot syndrome	0	0	0	0	0
Leukocytopenia	2 (10%)	0	0	0	2 (10%)
Aspartate transaminase increased	2 (10%)	2 (10%)	0	0	4 (20%)
Lipase increased	0	0	0	0	0
Proteinuria	0	0	0	0	0
Thrombocytopenia	2 (10%)	2 (10%)	0	0	4 (20%)
Vomiting	1 (5%)	3 (15%)	0	0	4 (20%)
Hypothyroidism	0	0	0	0	0
Triglycerides increased	0	0	0	0	0
Fatigue	6 (30%)	3 (15%)	0	0	9 (45%)
Blood bilirubin increased	0	0	2 (10%)	0	2 (10%)
Alanine transaminase increased	2 (10%)	1 (5%)	0	0	3 (15%)
Peripheral neurotoxicity	0	0	0	0	0
Hoarseness	0	0	0	0	0
Rash	4 (20%)	0	0	0	4 (20%)
Thyroiditis	0 (0%)	0	0	0	0
Diarrhea	1 (5%)	0	0	0	1 (5%)
Troponin increased	0	0	0	0	0
Fever	0	0	0	0	0
Alkaline phosphatase increased	0	0	0	0	0
Amylase increased	0	0	0	0	0
Hypertension	0	0	0	0	0

Table 3: Treatment-emergent adverse events (TEAEs) since the initiation of protocol-specified treatment

Identification of differentially expressed genes between responder and non-response groups

To elucidate the impact of the tumor immune microenvironment on combination therapy outcomes, we employed NanoString assay for transcriptome analysis of tumor samples obtained from 16 enrolled patients before and after treatment, totaling 32 samples (**Figure 3A**). Patients were stratified into r responder (PR) and non-responder (non-PR) groups based on treatment outcomes. Gene expression differential analysis between pre- and post-treatment samples within each group identified significant alterations, detailed in the **Supplementary Data** and illustrated in **Figure 3B.**

Our findings highlighted notable up-regulation of key genes involved in antigen presentation (CD40, TNFSF18, TNFSF4), immune checkpoint modulation (PDCD1LG2, CD274, IDO1, VTCN1), and T cell activation pathways (TNFRSF9, CD28, ICOS, CD40LG, CD2, GZMK, ENTPD1, ITGAE) in the responder group. Additionally, a diverse array of chemokine family genes (IL2, IL4, IL17A, CCR2, CCL22) showed enhanced expression in PR group (**Figure 3B**). Furthermore, immune cell abundance analysis based on 11 predefined immune cell types revealed significantly elevated levels in the PR group compared to non-PR. included T cells, B cells, mast cells, macrophages, Dendritic Cell (DC), Cytotoxic cells, NK CD56 cell, CD8 T cell, CD45 cell, Th1 cells and NK cell (**Figure 3C**). This heightened immune activation in responders encompassed robust antigen presentation, T cell activation, and co-stimulation processes crucial for effective immune-mediated tumor control.

Following the combination of stereotactic radiotherapy and immunotherapy, a striking reduction in

liver metastasis target lesions was observed in two patients compared to baseline To elucidate these findings, we conducted CD8 and PD-L1 immunohistochemical staining on liver metastasis biopsy specimens from one patient pre- and post-treatment (**Fig 3D-E**). The analysis revealed increased infiltration of T cells and improved immune microenvironment following treatment, aligning with our prior analytical findings.

Additional immune signatures analysis in predicting tumor response

We conducted gene expression analysis based on 12 predefined gene sets associated with immunotherapy and prognosis (**Figure 4A**). Notably, samples from the responder group exhibited higher expression of immune activation related genes compared to the non-responder group, include effector T cells (T-eff), T cell-Inflamed, IFN-γ ，cytotoxic, Cytolytic activity score (CYT), chemokines, angiogenesis (AG), APC co-stimulation (APC co-sti), inflammation promoting (Inflam-pro), T cell co-stimulation (T cell co-sti), parainflammation (parainflam) and tumor-infiltrating lymphocytes (TIL) (**Figure 4A**).

Further compared the related-signature score, we found the responders had higher APC and T cell co-stimulation signature scores compared with the non-responder group (**Figure 4B**). Moreover, the responders had higher T cell-Inflamed, inflammation promoting and parainflammation signature scores compared with the non-responder group (**Figure 4C**). Additionally, increased expression of effector T cell, cytotoxicity, IFN-γ production, and cytolytic activity and TIL signature scores compared with the non-responder group (**Figure 4D**).

Further functional insights into differential gene expression between responder and non-responder groups were gained through gene ontology (GO) enrichment and Kyoto Encyclopedia of Genes and Genomes (KEGG) pathway analyses. GO analysis highlighted enrichment in cytokine and chemokine receptor activities, alongside increased T cell and leukocyte proliferation and activation levels in responders (**Supplementary Fig 1A**). Correspondingly, KEGG analysis underscored enrichment in pathways involving antigen processing and presentation, T cell receptor signaling, chemokine interactions, and cytokine signaling (**Supplementary Fig 1B**). Notably, these results indicated responders after combination of Gamma Knife SBRT and tislelizumab treatment will enhancing tumor antigen presentation and T cell mediated immune response in pMMR/MSS/MSI-L mCRC.

Analysis on differential expression genes before and after treatment in the responders.

To unravel the mechanisms driving tumor regression in the responder cohort, we conducted comprehensive gene expression analysis before and after treatment, focusing on 7 gene groups known for their potential inhibitory effects on immunotherapy. Post-treatment analysis revealed significant reductions in exhausted T cells, Th2 cells, and Treg cells, indicative of a favorable shift away from a suppressive immune microenvironment (**Figure 5A**). Tumor resistance mechanisms, such as fibrosis and angiogenesis, play pivotal roles in limiting therapeutic efficacy(20,21). Initially, evaluation of immunotherapy-related gene groups in partial responders versus non-responders highlighted significantly higher angiogenesis scores in the former, albeit with no significantly difference (**Figure 5B**). Recognizing potential biases from pooling samples pre- and post-treatment, we conducted separate analyses within the responder group, expanding our gene set to include

fibrosis-related genes. The findings underscored substantial inhibition of both angiogenesis and fibrosis within the tumor microenvironment following SBRT, targeted therapy, and immunotherapy (**Figure 5C**).

Further stratified analysis of non-responder samples before and after treatment revealed no significant alterations in the expression levels of immunosuppression-related or angiogenesis/fibrosis-related gene sets (**Supplementary Fig 2**). These insights illuminate critical pathways through which combined therapies modulate the immune landscape and enhance treatment responses in pMMR/MSS/MSI-L mCRC.

Discussion:

By successfully reaching its main endpoint, this phase II trial shows that for combined Gamma Knife SBRT with tislelizumab greatly increases progression-free survival (PFS) in pMMR/MSS/MSI-L mCRC, resistant to first and second-line therapies. For this patient population, the combo treatment has shown both safety and tolerability. By overcoming resistance to first treatment plans, our study presents a creative therapy approach for those unresponsive to conventional treatments that offers a suitable therapeutic option improving clinical outcomes.

Among the several cancers including nasopharyngeal carcinoma, esophageal cancer, liver cancer, and lung cancer, Tislelizumab, a new PD-1 inhibitor, has been shown especially therapeutic efficacy. Combining tislelizumab with chemotherapy has essentially extended PFS in patients across these cancers (22-25).While immunotherapy has proven beneficial for some patients, metastatic colorectal

cancer (mCRC) presents unique challenges. Particularly in patients with MSS/pMMR tumors, which are marked by low immunogenicity and great resistance to immunotherapy, tumor cells in mCRC often evade immune detection and destruction (26). By directly targeting and destroying tumor cells, Gamma Knife SBRT presents a potential solution by releasing a significant volume of tumor neoantigens, and improving tumor immunogenicity, so optimizing maximizing the efficacy of subsequent immunotherapy(27). Furthermore demonstrated to extend survival in non-small cell lung cancer (NSCLC) with patients with brain metastases is the combination of Gamma Knife SBRT and immunotherapy (28). Still underreported, though, is the possibility of Gamma Knife SBRT coupled with ICIs to improve the response in pMMR/MSS/MSI-L CRC.

In our clinical observations, a notable therapeutic effect was achieved in a patient treated with combined SBRT and immunotherapy. We hypothesize that the addition of tislelizumab following SBRT could extend progression-free survival (PFS) compared to either modality alone. Tumor microenvironment post-radiotherapy showed significant changes revealed by sequencing analysis of tumor samples ‘both before and after combined treatment. More precisely, the microenvironment transitioned from an immunosuppressive, angiogenesis- and fibrosis-promoting state to an immune-enhanced, angiogenesis- and fibrosis-attenuated state. Comparatively to non-responders, responders expressed genes linked to antigen presentation, tumor inflammation, and immune-mediated tumor killing more strongly. Further showing the activation of several signaling pathways associated with tumor cell death, including NF-κB, TNF, and JAK-STAT pathways was enrichment analysis. Furthermore, immunotherapy targets such as PD-L1, showed an elevation, which supports the possibility of efficient later immunotherapy. These findings substantiate our

hypothesis that patients with MSS-type mCRC resistant to first-line treatment could benefit significantly from the combination of stereotactic radiotherapy and immunotherapy, with enhanced immunogenicity and a more favorable tumor microenvironment facilitating improved therapeutic outcomes.

This trial restrictions even if its outcomes show promise. First of all, our results could be biased as a single-arm study devoid of a control group. Second, the limited sample size and single-center design of the study lower its statistical power hence more robust conclusions depend on bigger studies. Furthermore, even though general survival (OS) was examined, the follow-up duration was insufficient to establish a reliable median OS. To address these limitations, a multi-center, randomized controlled trial with a larger cohort and extended follow-up period is essential. This will provide a more comprehensive evaluation of the efficacy and safety of combining Gamma Knife SBRT and tislelizumab as a later-line therapy in pMMR/MSS/MSI-L mCRC patients.

Ultimately, for patients with pMMR/MSS/MSI-L mCRC who were unresponsive to first-line therapy regimens, the combination of Gamma Knife SBRT with tislelizumab demonstrated a high disease control rate (DCR) and manageable safety profile. Significant post-radiotherapy improvements in the tumor's suppressive immune microenvironment, reduced fibrosis, normalized tumor vasculature, and activation of the PD-1/PD-L1 checkpoint pathway revealed by biomarker analyses so improving the efficacy of immunotherapy.

Methods

Study design and participants

This single-arm, phase II trial was conducted at the First Affiliated Hospital of Jinan University to assess the antitumor efficacy and safety of a combined regimen consisting of SBRT and tislelizumab in patients with pMMR/MSS/MSI-L-type metastatic colorectal cancer (mCRC). The study is registered with ClinicalTrials.gov (identifier: ChicTR2200011777). Eligible patients, aged 18-75 years, had confirmed metastatic colorectal cancer. MSS and RAS mutation statuses were determined through gene sequencing, while clinical staging was based on imaging examinations and intraoperative findings. A total of 20 patients were enrolled in the study, with all providing written informed consent. Detailed inclusion and exclusion criteria are available in the **Supplementary Materials**.

Procedures：

As illustrated in **Figure 1A**, eligible patients received SBRT (administered 5-6 times per week, 3-5 Gy per session) combined with tislelizumab (200 mg on day 1) was incorporated into the treatment regimen. Each three-week cycle comprised a maximum of 12 cycles of induction therapy. Patients achieving complete response (CR), partial response (PR), or stable disease (SD) transitioned to tislelizumab maintenance therapy (200 mg on day 1) until documented disease progression, death, unacceptable toxicity, or patient withdrawal of consent. Treatment response was evaluated using CT or MRI after each treatment cycle. Adverse events were systematically monitored and graded according to the National Cancer Institute Common Terminology Criteria for Adverse Events (version 5.0).

The study enrolled 20 eligible patients on November 24, 2022 (Figure 1B). All patients received at least one dose of the prescribed regimen. As of the data cutoff date (July 24, 2024), six patients continued to receive maintenance therapy. The median follow-up duration was 15 months (range: 3.4-20.0 months, IQR: 9.6-18.2 months). Due to disease-related complications, specimens could not be obtained from four patients, resulting in 16 patients being included in the per-protocol set (PPS).

Outcomes：

The primary endpoints of the study were objective response rate (ORR) and safety, encompassing adverse events and serious adverse events, assessed according to RECIST version 1.1. Secondary endpoints included disease control rate (DCR) and progression-free survival (PFS). ORR was defined as the proportion of patients who achieved a best objective response of complete response (CR) or partial response (PR) per RECIST criteria (version 1.1). DCR was defined as the proportion of patients who achieved CR, PR, or stable disease (SD) according to RECIST criteria (version 1.1). PFS was defined as the time from enrollment to the first documented disease progression per RECIST version 1.1 or to death from any cause, whichever occurred first.

CD8 & PD-L1 expression level：

Tumoral CD8 & PD-L1 expression was measured by immunohistochemistry (IHC) (22C3 pharmDx assays). The sections were scored for staining intensity according to the following scale: 0 (no staining), 1 (weak staining, light yellow), 2 (moderate staining, yellowish brown), and 3 (strong staining, brown), with 0 and 1 considered low expression, and 2 and 3 considered high expression. The score is divided into 4 levels according to the percentage of positive cells: 0%≤positive cell percentage≤25%, 1 point; 25%<positive cell percentage≤50%, 2 points; 50%<positive cell percentage≤75%, 3 points; 75%<positive cell percentage≤100%, 4 points. IHC score = cell staining intensity score x positive cell percentage score. The PD-L1 combined positive score (CPS) was defined as the number of PD-L1 positive cells (tumor cells, lymphocytes, macrophages) as a proportion of the total number of tumor cells multiplied by 100. Positive PD-L1 expression was considered when the CPS was >1.

Nanostring panel RNA sequencing：

Due to disease-related limitations, specimens could not be obtained from four patients, resulting in a cohort of 16 patients for combined analysis. Tumor tissue samples were collected both before treatment (BT) and after treatment (AT). Gene expression of each sample was measured using the

NanoString nCounter platform (NanoString Technologies, Seattle, WA). The quantitative transcriptome data were obtained based on the 289-immuno-gene panel, which includes 289 genes related to the tumor, tumor microenvironment, and immune responses in cancer. The samples that passed the quality control (QC), which included Imaging QC, Binding Density QC, Positive Control Linearity QC, and Positive Normalization QC can be processed in further analysis. The raw count data of 289 genes were normalized using the R package NanoStringNorm according to the geometric mean of five housekeeping genes. The log2 transformation was then performed on the normalized data. Differentially expressed genes were identified using the "DEseq2" package, employing criteria of log2|fold change| > 1 and false discovery rate < 0.05. Heatmaps depicting the expression patterns of these differentially expressed genes were generated using the "ComplexHeatmap" package.

Immune cell profile analyses and Additional immune signatures analysis

The determination of immune cell types and gene sets associated with immunotherapy response was informed by established literature sources (29,30). We transformed each attribute (immune signature or gene set) value (GSVA score) xi into xi′ by the equation xi′ □=□(xi□−□xmin)/(xmax□−□xmin), where xmin and xmax represent the minimum and maximum of the ssGSEA scores for the gene set across all samples, respectively. The detailed gene signature list can be found in the **Supplementary Table**.

Gene set enrichment and pathway analysis

The Kyoto Encyclopedia of Genes and Genomes (KEGG) / Gene Ontology (GO) enrichment analysis was performed using the Clusterprofiler R package. The list of gene IDs was used as the input file. The Benjamini-Hochberg method was employed to adjust the p-values. The cut-off threshold of p-values was set to 0.05. The enrichment results were visualized by the ggplot2 R package. The enrichment statistic was set to classic.

Statistical analyses

Progression-free survival (PFS) and OS was estimated utilizing the Kaplan-Meier method. Statistical analyses were conducted using R (version 3.6.1). Differences between subgroups in terms of efficacy response were assessed using the nonparametric Wilcoxon rank-sum test (Mann-Whitney U test), while comparisons between pre- and post-treatment samples were analyzed with the Wilcoxon signed-rank test. Confidence intervals (CIs) for response rates were calculated employing the Clopper-Pearson method, with all reported P values being two-sided. A P value < 0.05 was considered statistically significant.

Data availability

The data generated in this study are available within the article and its **Supplementary Data**. Additional data or resources related to this article are available upon reasonable request from the corresponding authors.

Acknowledgments

This research was supported by the Clinical Frontier Technology Program of the First Affiliated Hospital of Jinan University (No. JNU1AF-CFTP-2022-a01223), the National Natural Science Foundation of China (82204436), Natural Science Foundation of Guangdong Province (2024A1515030010, 2022A1515011695), Science and Technology Projects in Guangzhou (2024A03J0825).

Ethics approval and consent to participate

This trail was conducted in accordance with the Declaration of Helsinki after approval by the Institutional Review Board of The First Affiliated Hospital of Jinan University (KY-2022-236). All patients provided written informed consent. The ClinicalTrials.gov identifier was: ChiCTR2200066117.

Author Contributions

Y Zhang, H Guan and S Liu: acquisition of data, analysis of experimental data and drafted the manuscript. H Li and Z Bian: Investigation, visualization and methodology. J He, Z Zhao and S Qiu: data curation, software and formal analysis. T Mo, X Zhang and Z Chen: technical expertise inmanuscript editing. H Ding and X Zhao: assay optimization, acquisition, and analysis and interpretation of histology and pathology. L Wang, Y Pan and J Pan: funding acquisition, designed the study and writing-review and editing the draft.

References

1. Sung H, Ferlay J, Siegel RL, Laversanne M, Soerjomataram I, Jemal A, *et al.* Global Cancer Statistics 2020: GLOBOCAN Estimates of Incidence and Mortality Worldwide for 36 Cancers in 185 Countries. CA: a cancer journal for clinicians **2021**;71(3):209-49 doi 10.3322/caac.21660.
2. Siegel RL, Miller KD, Goding Sauer A, Fedewa SA, Butterly LF, Anderson JC, *et al.* Colorectal cancer statistics, 2020. CA: a cancer journal for clinicians **2020**;70(3):145-64 doi 10.3322/caac.21601.
3. Biller LH, Schrag D. Diagnosis and Treatment of Metastatic Colorectal Cancer: A Review. Jama **2021**;325(7):669-85 doi 10.1001/jama.2021.0106.
4. Diagnosis, Treatment Guidelines For Colorectal Cancer Working Group C. Chinese Society of Clinical Oncology (CSCO) diagnosis and treatment guidelines for colorectal cancer 2018 (English version). Chinese journal of cancer research = Chung-kuo yen cheng yen chiu **2019**;31(1):117-34 doi 10.21147/j.issn.1000-9604.2019.01.07.
5. Benson AB, Venook AP, Al-Hawary MM, Arain MA, Chen YJ, Ciombor KK, *et al.* Colon Cancer, Version 2.2021, NCCN Clinical Practice Guidelines in Oncology. Journal of the National Comprehensive Cancer Network : JNCCN **2021**;19(3):329-59 doi 10.6004/jnccn.2021.0012.
6. Cox AD, Fesik SW, Kimmelman AC, Luo J, Der CJ. Drugging the undruggable RAS: Mission possible? Nature reviews Drug discovery **2014**;13(11):828-51 doi 10.1038/nrd4389.
7. Modest DP, Ricard I, Heinemann V, Hegewisch-Becker S, Schmiegel W, Porschen R, *et al.* Outcome according to KRAS-, NRAS- and BRAF-mutation as well as KRAS mutation variants: pooled analysis of five randomized trials in metastatic colorectal cancer by the AIO colorectal cancer study group. Annals of oncology : official journal of the European Society for Medical Oncology **2016**;27(9):1746-53 doi 10.1093/annonc/mdw261.
8. Asaoka Y, Ijichi H, Koike K. PD-1 Blockade in Tumors with Mismatch-Repair Deficiency. The New England journal of medicine **2015**;373(20):1979 doi 10.1056/NEJMc1510353.
9. Ganesh K, Stadler ZK, Cercek A, Mendelsohn RB, Shia J, Segal NH, *et al.* Immunotherapy in colorectal cancer: rationale, challenges and potential. Nature reviews Gastroenterology & hepatology **2019**;16(6):361-75 doi 10.1038/s41575-019-0126-x.
10. Yi M, Zheng X, Niu M, Zhu S, Ge H, Wu K. Combination strategies with PD-1/PD-L1 blockade: current advances and future directions. Molecular cancer **2022**;21(1):28 doi 10.1186/s12943-021-01489-2.
11. Limagne E, Euvrard R, Thibaudin M, Rébé C, Derangère V, Chevriaux A, *et al.* Accumulation of MDSC and Th17 Cells in Patients with Metastatic Colorectal Cancer Predicts the Efficacy of a FOLFOX-Bevacizumab Drug Treatment Regimen. Cancer research **2016**;76(18):5241-52 doi 10.1158/0008-5472.Can-15-3164.
12. Hamid MA, Pammer LM, Lentner TK, Doleschal B, Gruber R, Kocher F, *et al.* Immunotherapy for Microsatellite-Stable Metastatic Colorectal Cancer: Can we close the Gap between Potential and Practice? Current oncology reports **2024** doi 10.1007/s11912-024-01583-w.
13. Antoniotti C, Rossini D, Pietrantonio F, Catteau A, Salvatore L, Lonardi S, *et al.* Upfront FOLFOXIRI plus bevacizumab with or without atezolizumab in the treatment of patients with metastatic colorectal cancer (AtezoTRIBE): a multicentre, open-label, randomised, controlled, phase 2 trial. The Lancet Oncology **2022**;23(7):876-87 doi 10.1016/s1470-2045(22)00274-1.
14. Papiez L, Timmerman R, DesRosiers C, Randall M. Extracranial stereotactic radioablation: physical principles. Acta oncologica (Stockholm, Sweden) **2003**;42(8):882-94 doi 10.1080/02841860310013490.
15. Mac Manus M, Lamborn K, Khan W, Varghese A, Graef L, Knox S. Radiotherapy-associated neutropenia and thrombocytopenia: analysis of risk factors and development of a predictive model. Blood **1997**;89(7):2303-10.
16. Singh AK, Winslow TB, Kermany MH, Goritz V, Heit L, Miller A, *et al.* A Pilot Study of Stereotactic Body Radiation Therapy Combined with Cytoreductive Nephrectomy for Metastatic Renal Cell Carcinoma. Clinical cancer research : an official journal of the American Association for Cancer Research **2017**;23(17):5055-65 doi

10.1158/1078-0432.Ccr-16-2946.

17. Choi CW, Jeong MH, Park YS, Son CH, Lee HR, Koh EK. Combination Treatment of Stereotactic Body Radiation Therapy and Immature Dendritic Cell Vaccination for Augmentation of Local and Systemic Effects. Cancer research and treatment **2019**;51(2):464-73 doi 10.4143/crt.2018.186.

18. Morinaga N, Tanaka N, Shitara Y, Ishizaki M, Yoshida T, Kouga H, *et al.* Ten-Year Survival of a Patient Treated with Stereotactic Gamma Knife Radiosurgery for Brain Metastases from Colon Cancer with Ovarian and Lymph Node Metastases: A Case Report. Case reports in gastroenterology **2016**;10(1):199-206 doi 10.1159/000445976.

19. Liu S, Zhang Y, Lin Y, Wang P, Pan Y. Case report: The MSI-L/p-MMR metastatic rectal cancer patient who failed systemic therapy responds to anti-PD-1 immunotherapy after stereotactic body radiation-therapy. Frontiers in immunology **2022**;13:981527 doi 10.3389/fimmu.2022.981527.

20. Herzog BH, Baer JM, Borcherding N, Kingston NL, Belle JI, Knolhoff BL, *et al.* Tumor-associated fibrosis impairs immune surveillance and response to immune checkpoint blockade in non-small cell lung cancer. Science translational medicine **2023**;15(699):eadh8005 doi 10.1126/scitranslmed.adh8005.

21. Kopecka J, Salaroglio IC, Perez-Ruiz E, Sarmento-Ribeiro AB, Saponara S, De Las Rivas J, *et al.* Hypoxia as a driver of resistance to immunotherapy. Drug resistance updates : reviews and commentaries in antimicrobial and anticancer chemotherapy **2021**;59:100787 doi 10.1016/j.drup.2021.100787.

22. Yang Y, Pan J, Wang H, Zhao Y, Qu S, Chen N, *et al.* Tislelizumab plus chemotherapy as first-line treatment for recurrent or metastatic nasopharyngeal cancer: A multicenter phase 3 trial (RATIONALE-309). Cancer cell **2023**;41(6):1061-72.e4 doi 10.1016/j.ccell.2023.04.014.

23. Wang J, Lu S, Yu X, Hu Y, Sun Y, Wang Z, *et al.* Tislelizumab Plus Chemotherapy vs Chemotherapy Alone as First-line Treatment for Advanced Squamous Non-Small-Cell Lung Cancer: A Phase 3 Randomized Clinical Trial. JAMA oncology **2021**;7(5):709-17 doi 10.1001/jamaoncol.2021.0366.

24. Shen L, Kato K, Kim SB, Ajani JA, Zhao K, He Z, *et al.* Tislelizumab Versus Chemotherapy as Second-Line Treatment for Advanced or Metastatic Esophageal Squamous Cell Carcinoma (RATIONALE-302): A Randomized Phase III Study. Journal of clinical oncology : official journal of the American Society of Clinical Oncology **2022**;40(26):3065-76 doi 10.1200/jco.21.01926.

25. Qin S, Kudo M, Meyer T, Bai Y, Guo Y, Meng Z, *et al.* Tislelizumab vs Sorafenib as First-Line Treatment for Unresectable Hepatocellular Carcinoma: A Phase 3 Randomized Clinical Trial. JAMA oncology **2023**;9(12):1651-9 doi 10.1001/jamaoncol.2023.4003.

26. Zhao W, Jin L, Chen P, Li D, Gao W, Dong G. Colorectal cancer immunotherapy-Recent progress and future directions. Cancer letters **2022**;545:215816 doi 10.1016/j.canlet.2022.215816.

27. Kievit H, Muntinghe-Wagenaar MB, Hijmering-Kappelle LBM, Hiddinga BI, Ubbels JF, Wijsman R, *et al.* Safety and tolerability of stereotactic radiotherapy combined with durvalumab with or without tremelimumab in advanced non-small cell lung cancer, the phase I SICI trial. Lung cancer (Amsterdam, Netherlands) **2023**;178:96-102 doi 10.1016/j.lungcan.2023.02.004.

28. Cho A, Untersteiner H, Hirschmann D, Shaltout A, Göbl P, Dorfer C, *et al.* Gamma Knife Radiosurgery for Brain Metastases in Non-Small Cell Lung Cancer Patients Treated with Immunotherapy or Targeted Therapy. Cancers **2020**;12(12) doi 10.3390/cancers12123668.

29. He Y, Jiang Z, Chen C, Wang X. Classification of triple-negative breast cancers based on Immunogenomic profiling. Journal of experimental & clinical cancer research : CR **2018**;37(1):327 doi 10.1186/s13046-018-1002-1.

30. Zeng TM, Yang G, Lou C, Wei W, Tao CJ, Chen XY, *et al.* Clinical and biomarker analyses of sintilimab plus gemcitabine and cisplatin as first-line treatment for patients with advanced biliary tract cancer. Nature communications **2023**;14(1):1340 doi 10.1038/s41467-023-37030-w.

505 **Figure legends**

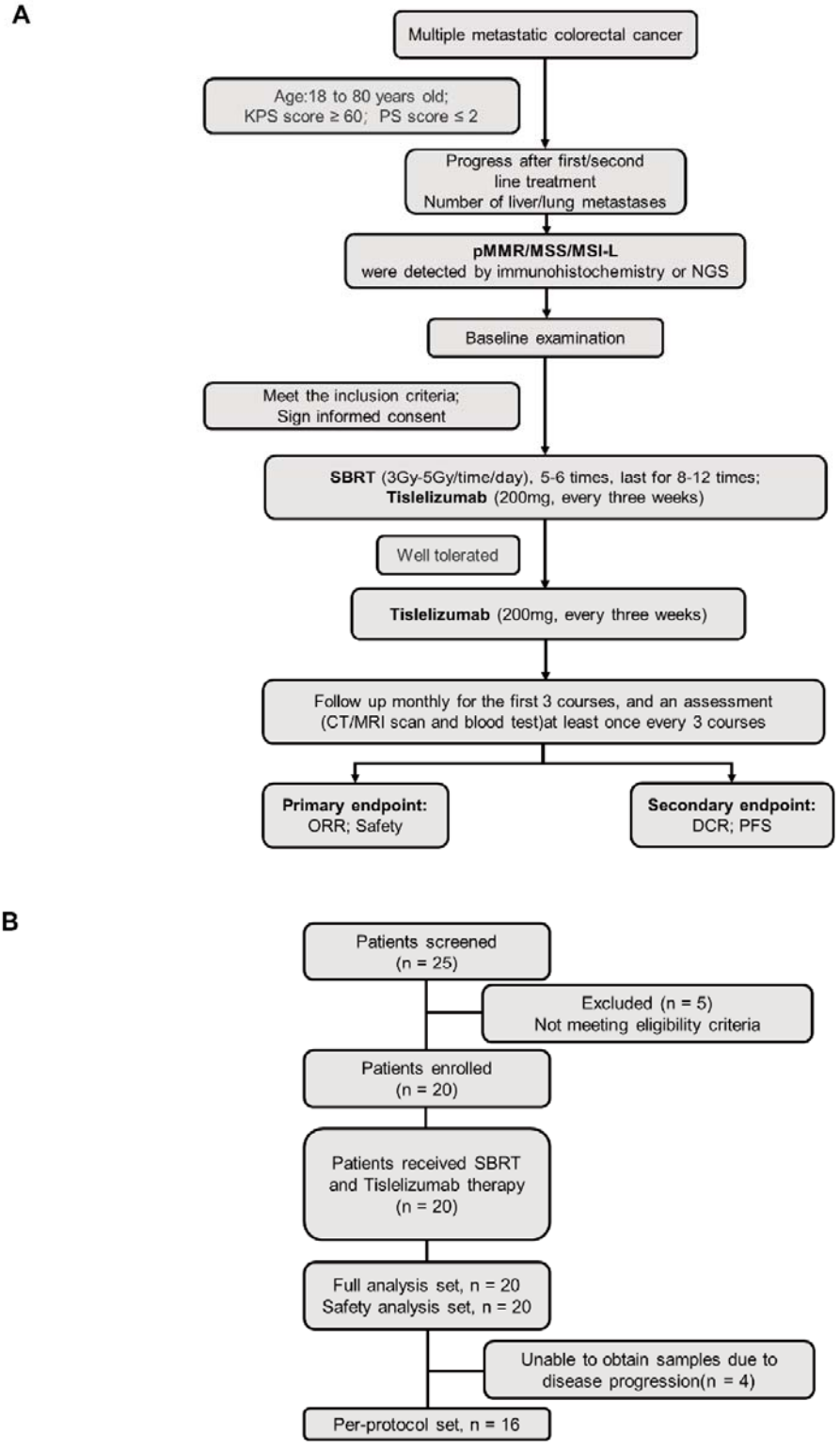

506

507 **Figure 1. Clinical trial flow chart. A)** Flowchart of therapeutic regimen. **B)** Flow diagram of participants in the

508 study.

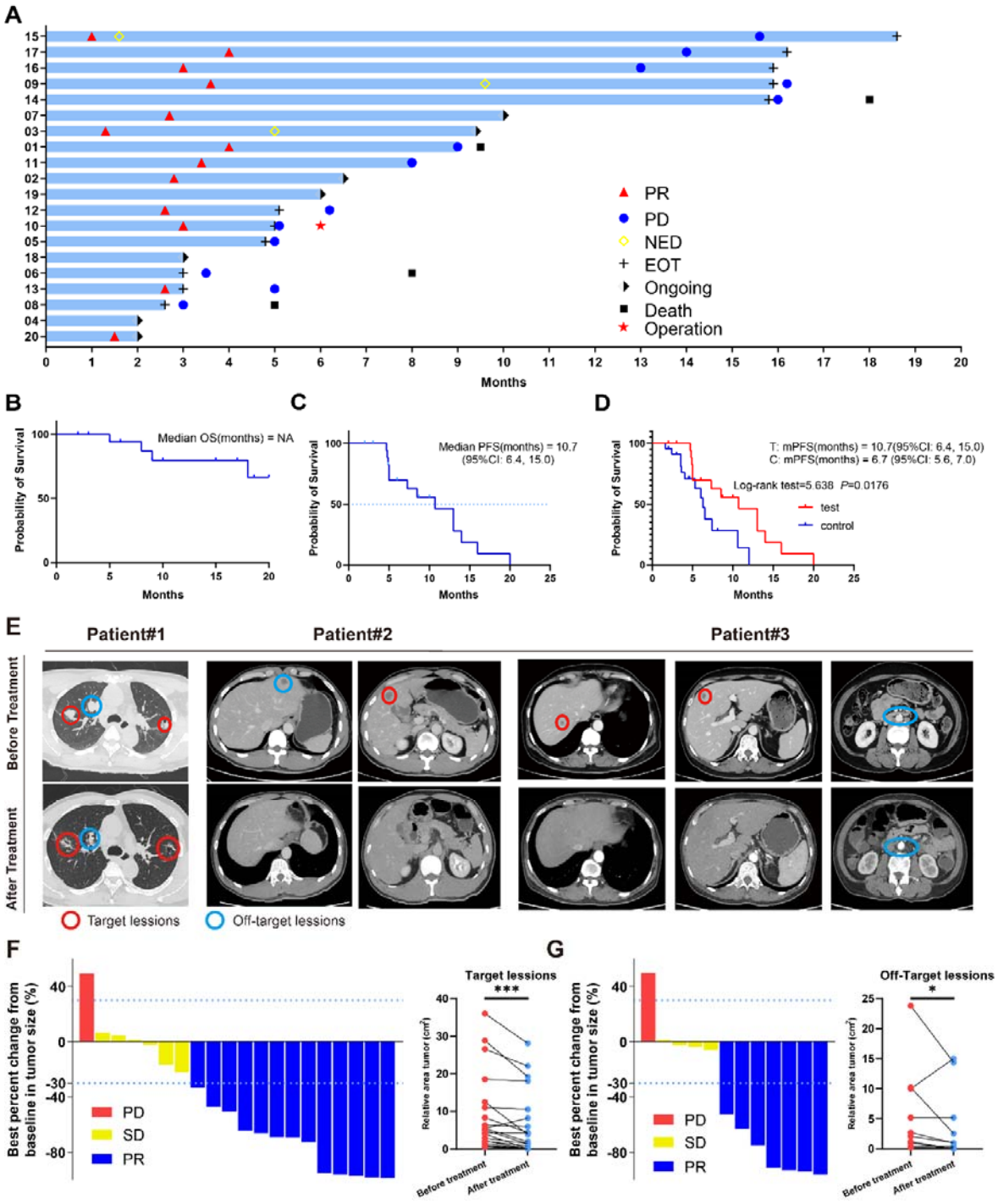

Figure 2. Clinical trial results. A) Swimmer plots of patients. **B)** Kaplan–Meier curves of OS for the per-protocol set (N = 20). **C)** Kaplan–Meier curves of PFS for the per-protocol set (N = 20). **D)** Kaplan–Meier curves of PFS for didn't receive immunotherapy set (control group) (N= 23) and per-protocol set (test group) (N=20). **E)** Radiological response from patient. **F)** Waterfall plot of best percent change from baseline in patient target lesion (N= 20). **G)** Waterfall plot of best percent change from baseline in patient off-target lesion (N= 12).

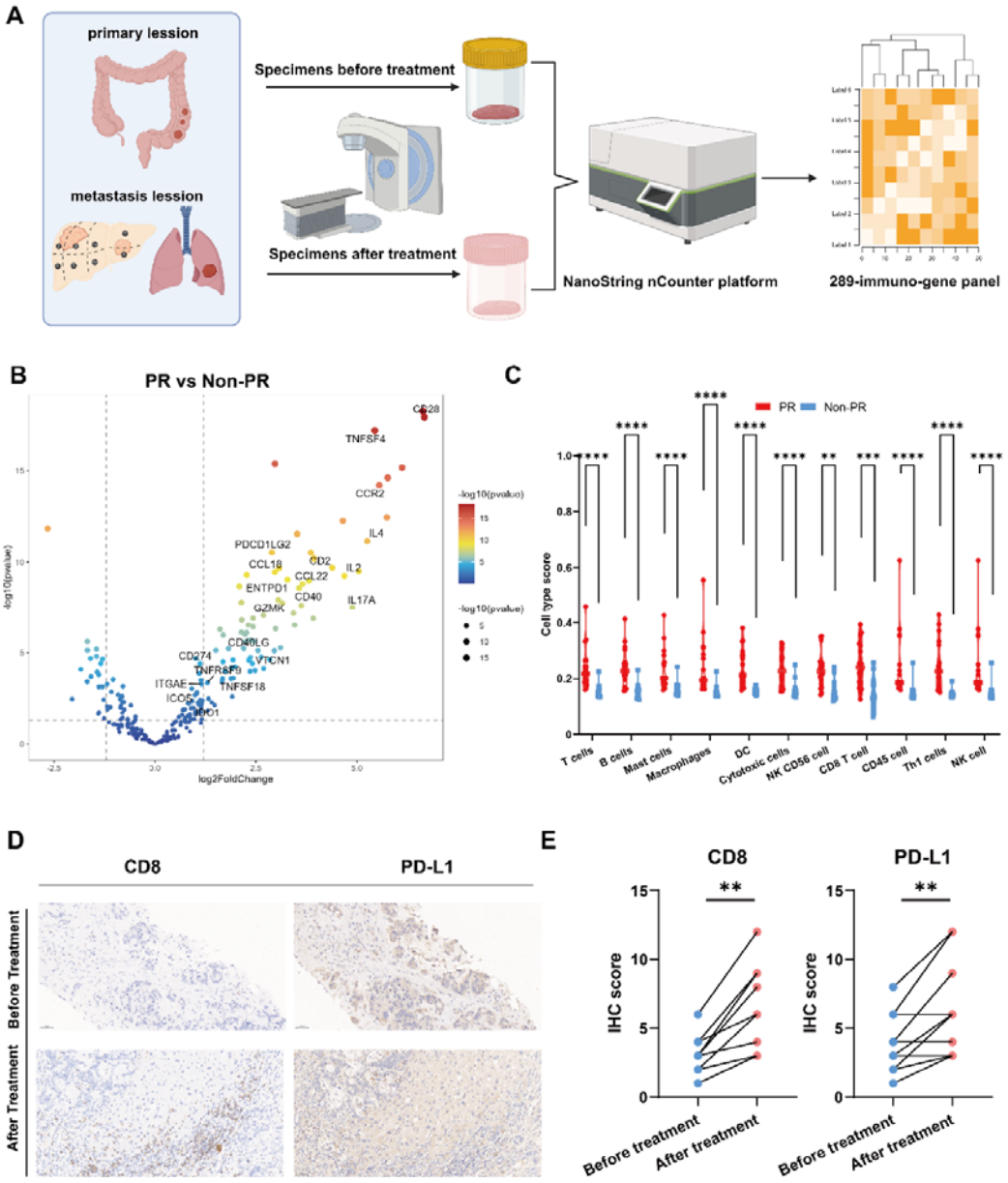

Figure 3. Differential expressed genes analysis. A) Specimens collection flowchart. **B)** Transcriptome analysis on differential expression genes before and after treatment between responders (PR) (n = 9) and non-responders (Non-PR) (n = 7), DESeq2 was provided to perform differential expression testing. **C)** The abundance of predefined 12 immune cells composition before and after treatment between responders (PR) (n = 9) and non-responders (Non-PR) (n = 7), Wilcoxon test was used to determine the statistical significance between subgroups. **D)** Radiological response from patient. **E)** Representative CD8 & PD-L1 IHC staining of before and after treatment specimens of patient**.**

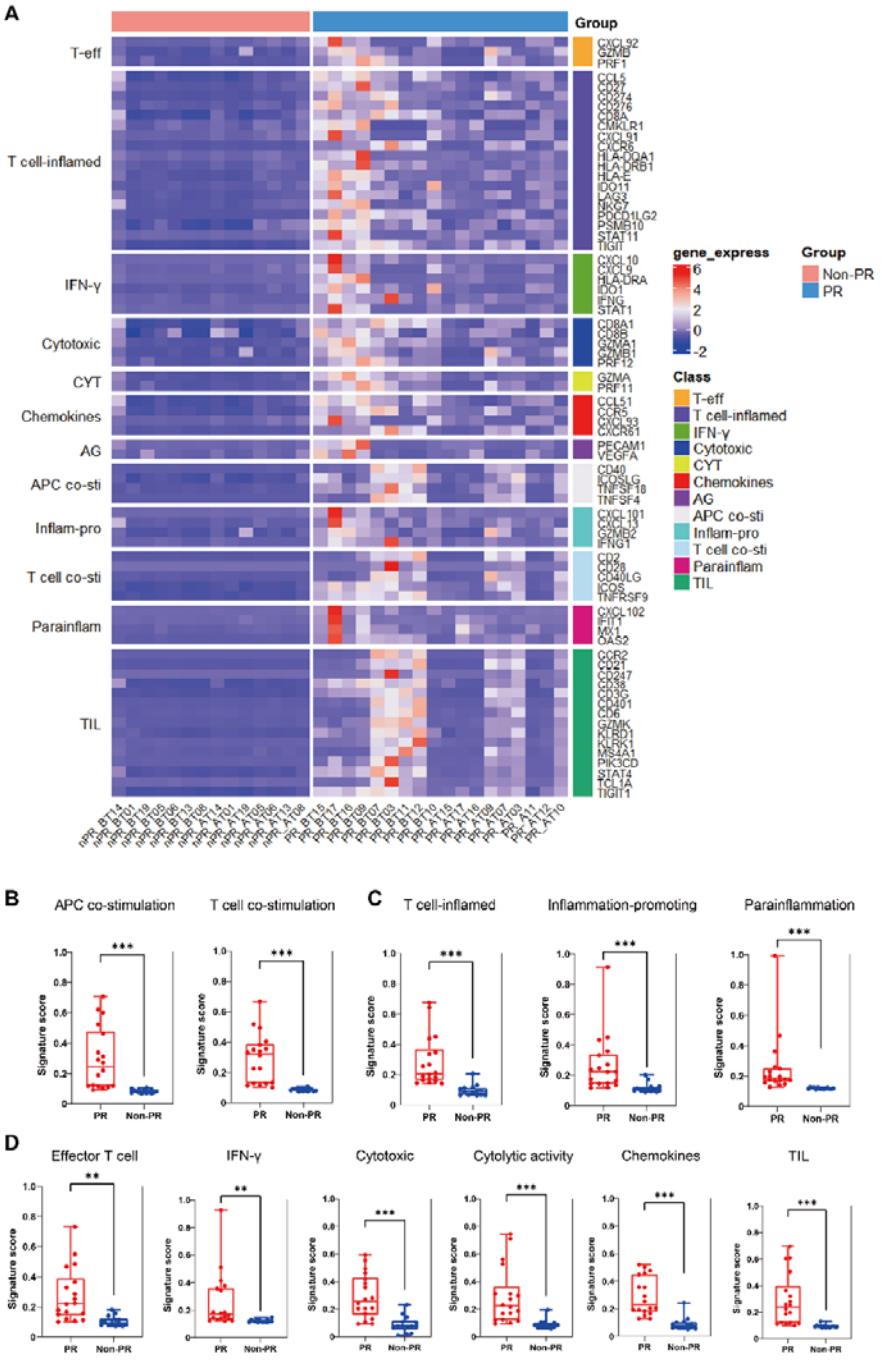

Figure 4. Additional immune signatures analysis. A) The expression of 12 gene sets previously reported to be associated with response to immunotherapy and prognosis between responders (PR) (n = 18) and non-responders (Non-PR) (n = 14). **BCD)** 11 gene sets of prognostic value were differentially expressed between responders (PR) (n = 18) and non-responders (Non-PR) (n = 14), box plots are indicated in terms of minima, maxima, centre, bounds of box and whiskers (interquartile range value), and percentile in the style of Tukey, Wilcoxon test was used to determine the statistical significance between subgroups.

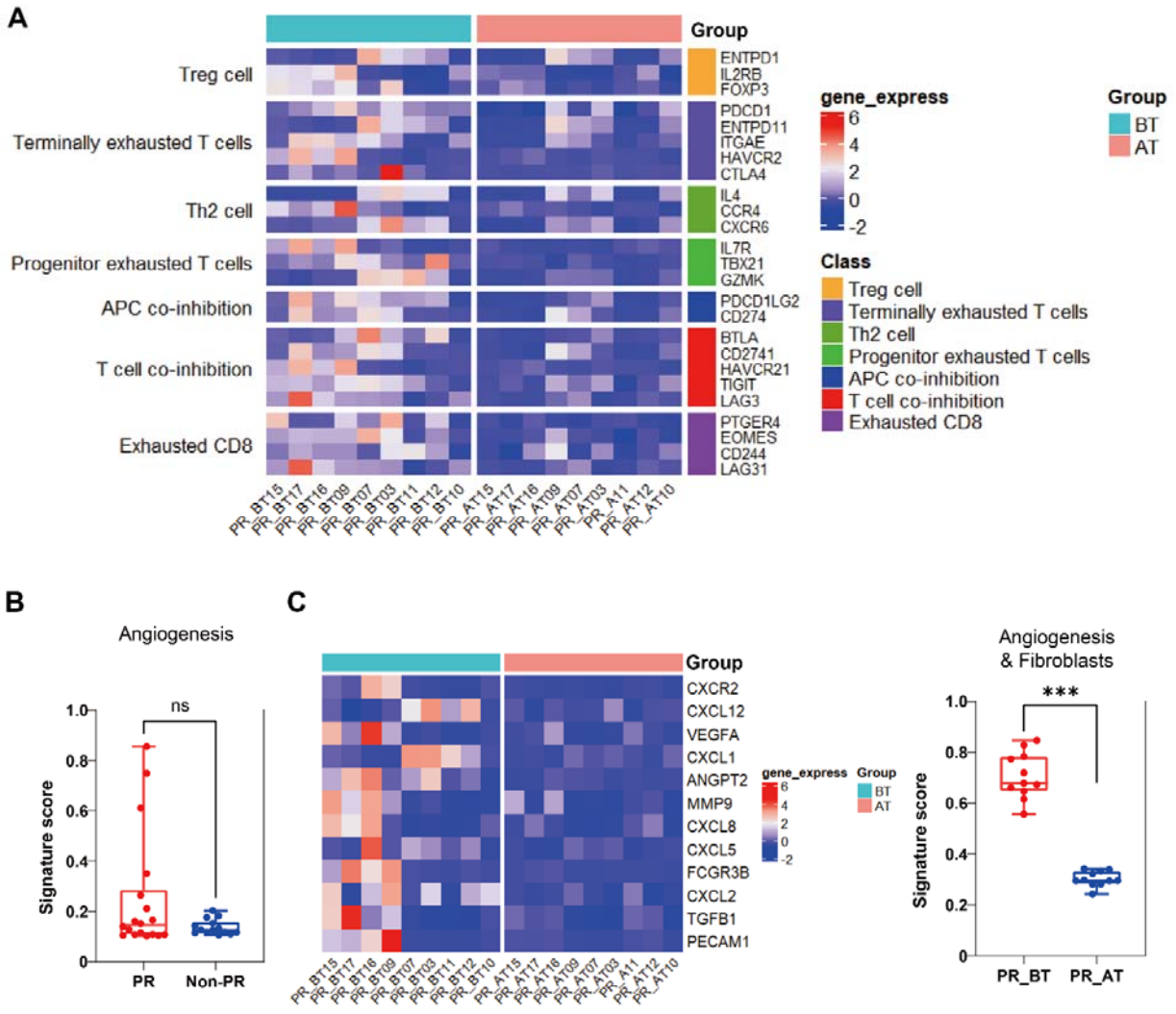

Figure 5. Comparison of responders before and after treatment A) The expression of 7 gene sets previously reported to be associated with response to immunosuppressive between before treatment (n = 9) and after treatment (n = 9) in the responders (PR). **B)** The expression of Angiogenesis sets between responders (PR) (n = 18) and non-responders (Non-PR) (n = 14). **C)** The expression of Angiogenesis & Fibroblasts sets between before treatment (n = 9) and after treatment (n = 9) in the responders. Box plots are indicated in terms of minima, maxima, centre, bounds of box and whiskers (interquartile range value), and percentile in the style of Tukey, Wilcoxon test was used to determine the statistical significance between subgroups.

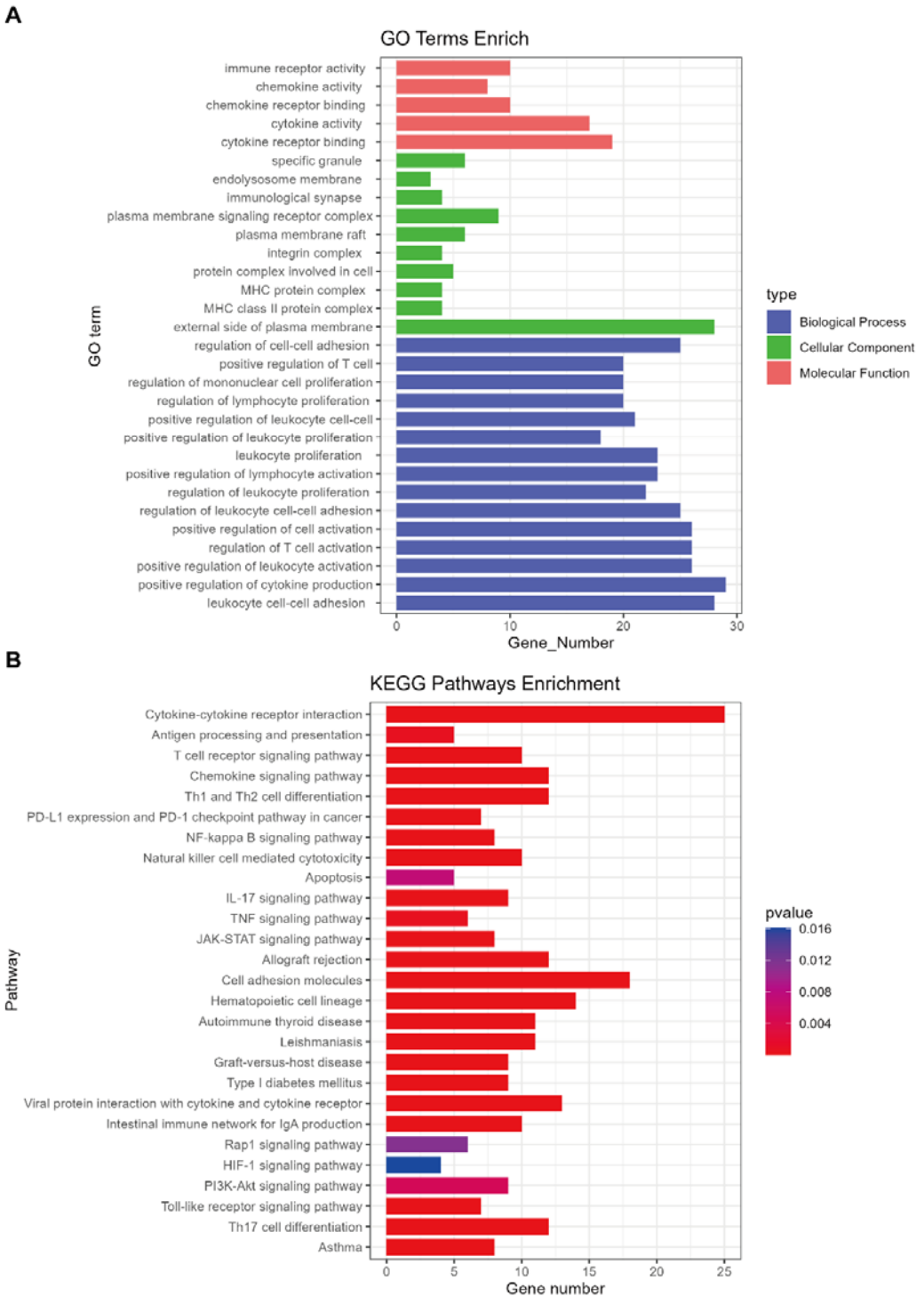

Supplementary Figure1. GO enrichment and KEGG pathways analysis of differential expression genes. **A)** GO enrichment analysis were performed to identify the biological process, cellular component and molecular function of differential expression genes. **B)** H KEGG enrichment analysis of differential expression genes.

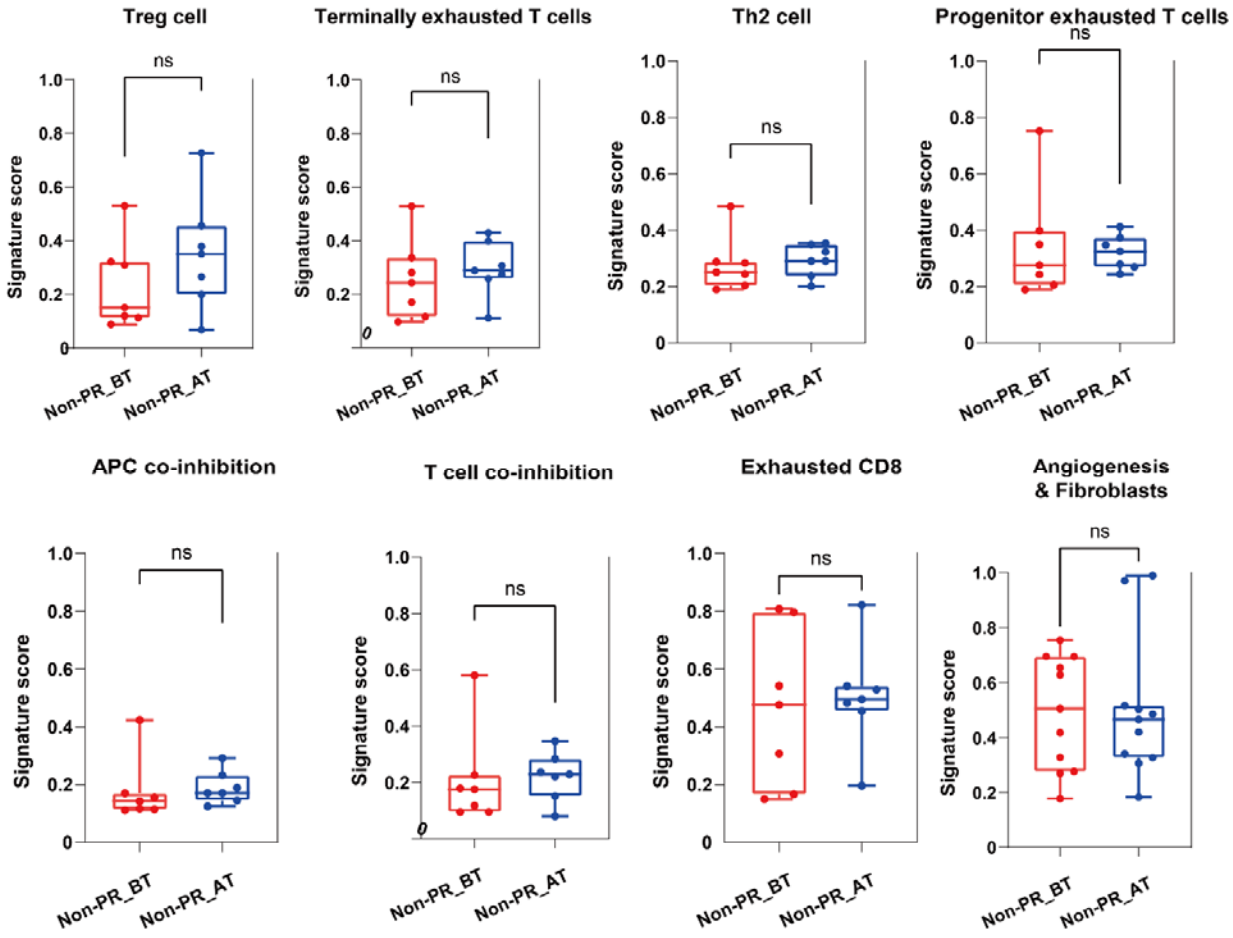

Supplementary Figure2. Comparison of non-responders before and after treatment.